CrossMark

EXPERIMENTAL RESEARCH - VASCULAR

Leukocyte plugging and cortical capillary flow after subarachnoid hemorrhage

Mami Ishikawa[1,2] · **Mayumi Kajimura**[2] · **Takayuki Morikawa**[2,3] · **Kosuke Tsukada**[4] ·
Toshiyuki Tsuji[2] · **Gen Kusaka**[1] · **Yuichi Tanaka**[1] · **Makoto Suematsu**[2]

Abstract

Background It is believed that increased intracranial pressure immediately after subarachnoid hemorrhage (SAH) causes extensive brain ischemia and results in worsening clinical status. Arterial flow to the cerebral surfaces is clinically well maintained during clipping surgery regardless of the severity of the World Federation of Neurological Societies grade after SAH. To explore what kinds of changes occur in the cortical microcirculation, not at the cerebral surface, we examined cortical microcirculation after SAH using two-photon laser scanning microscopy (TPLSM).

Methods SAH was induced in mice with an endovascular perforation model. Following continuous injection of rhodamine 6G, velocities of labeled platelets and leukocytes and unlabeled red blood cells (RBCs) were measured in the cortical capillaries 60 min after SAH with a line-scan method using TPLSM, and the data were compared to a sham group and P-selectin monoclonal antibody-treated group.

Results Velocities of leukocytes, platelets, and RBCs in capillaries decreased significantly 60 min after SAH. Rolling and adherent leukocytes suddenly prevented other blood cells from flowing in the capillaries. Flowing blood cells also decreased significantly in each capillary after SAH. This no-reflow phenomenon induced by plugging leukocytes was often observed in the SAH group but not in the sham group. The decreased velocities of blood cells were reversed by pretreatment with the monoclonal antibody of P-selection, an adhesion molecule expressed on the surfaces of both endothelial cells and platelets.

Conclusions SAH caused sudden worsening of cortical microcirculation at the onset. Leukocyte plugging in capillaries is one of the reasons why cortical microcirculation is aggravated after SAH.

Keywords No reflow · Cerebral microcirculation · Two photon · Line scan · P-selectin

✉ Mami Ishikawa
  m.ishikawa@jichi.ac.jp

1 Department of Neurosurgery, Saitama Medical Center, Jichi Medical University, 1-847 Amanumacho Omiya-ku,
  Saitama-city, Saitama 330-8503, Japan

2 Department of Biochemistry School of Medicine, Keio University,
  Tokyo, Japan

3 Department of Stem Cell Biology, Research Institute, National
  Center for Global Health and Medicine, Tokyo, Japan

4 Graduate School of Science and Technology, Keio University,
  Kanagawa, Japan

Introduction

Subarachnoid hemorrhage (SAH) increases intracranial pressure (ICP), decreases cerebral blood flow (CBF), and results in acute brain injury, which worsens a patient's clinical status at the onset. This process has also been induced by puncture or injury of a cerebral artery in animal SAH models. These direct puncture or injury models represent actual acute clinical flow dynamics after SAH. Using these models, acute brain injury and cerebral microcirculation have been investigated [2, 3, 8, 9, 12, 13, 20, 22, 24, 25, 30, 31, 36, 37].

Using a carbon black method as an indicator of blood flow, Asano [2] proposed the pathogenetic role of the no-reflow phenomenon in intraparenchymal capillary networks during the acute stage of SAH induced by injury of the internal

carotid artery using a lateral skull base approach. This no-reflow phenomenon had already been proposed as a pathogenetic mechanism of postischemic injury [1], and Villringer et al. [39] first observed intracapillary leukocyte plugging in a model of global cerebral ischemia. However, Dirnagl et al. [7] reported that leukocyte plugging was not responsible for early cortical hypoperfusion after brief global ischemia in rats. The no-reflow phenomenon was one of the important pathophysiologic mechanisms of cerebral ischemia, but it was still not clear whether leukocytes really obstructed capillaries. Recently, using two-photon laser scanning microscopy (TPLSM), it was reported that flow stagnation because of leukocyte plugging was frequently observed in the cortical capillaries [40]. On the other hand, the no-reflow phenomenon after SAH has been discussed as a mechanism of acute brain injury [2, 37, 38], but has never been demonstrated in SAH models in vivo. We have reported platelet-leukocyte-endothelial cell interactions in venules on the cerebral surface at 2 h after SAH induction [20]. Microvascular constriction 3 h after SAH has also been reported [8]. These microcirculatory changes in the acute phase of SAH have been examined on the cerebral surface, not in the cortex, because observation of the cortical microcirculation immediately after SAH is technically difficult.

Therefore, we have created an experiment with a line-scan method using TPLSM to record and analyze cortical flow dynamics after SAH. The cortical microcirculation was first observed in vivo after SAH using TPLSM with line-scan analysis and comparing data obtained before SAH in order to elucidate the underlying pathophysiology of acute brain injury after SAH.

Materials and methods

Animal preparations

Experiments were performed using male mice [FVB/N-Tg(GFAPGFP)14Mes/J] weighing 25–28 g to identify an astrocyte and its end foot around a precapillary arteriole. The animals were anesthetized with an intraperitoneal injection of alpha-chloralose (60 mg/kg) and urethane (600 mg/kg), while lidocaine (1 %) was employed for local anesthesia. All mice were tracheostomized with a polyethylene catheter (PE-90, Intramedic, Clay Adams, Parsippany, NJ) and allowed to breathe spontaneously. The femoral artery and vein were cannulated with polyethylene catheters (PE-10, Intramedic, Clay Adams, Parsippany, NJ) to monitor mean arterial blood pressure and sample arterial blood for blood gas analysis and for intravenous administration of Qdot 655® or rhodamine 6G (Sigma-Aldrich Chemicals, St. Louis, MO). Rectal temperature was monitored and maintained at 36.5–37.5 °C using a heating pad throughout the experimental procedure.

Cranial window

The head of each mouse was fixed with a stereotactic frame in the sphinx position (SG-4 N, Narishige Scientific Instrument Lab, Tokyo, Japan). The skull bone was exposed by a midline skin incision, followed by a craniectomy (diameter, 2 mm) using a drill at the parietal bone. The dura mater was not cut. A 12-mm glass coverslip was placed over the craniectomy field, and the space between the glass and dura mater was filled with phosphate-buffered saline (PBS). To record clear fluorescent images, we used a water immersion objective. Distilled water on the objective side and PBS on the skull side were separately maintained by a 12-mm-wide glass, which was put on the exposed skull and kept in place during observations without being tightly fixed.

SAH model

Using an endovascular perforation model [3, 20], SAH was induced in the supine position. After a midline neck incision, the left external carotid artery (ECA) and pterygopalatine artery were isolated and ligated. After the left internal carotid artery (ICA) was exposed and dissected free from the common carotid artery (CCA) to the basal cranium, the CCA was ligated with silk sutures. After occlusion of the ICA using a microvascular clip (#15911, World Precision Instruments, Sarasota, FL) at the pterygopalatine bifurcation, a suture was inserted from the left ECA and advanced to the carotid bifurcation. The tip of a 6–0 nylon monofilament was blunted to 0.21 mm in diameter with a coagulator. The ECA was then cut and rotated with the nylon thread to further advance the nylon thread into the ICA after removal of the microvascular clip at the ICA. The nylon thread was advanced more than 10 mm from the carotid bifurcation to further perforate the cerebral artery. This procedure was performed once to generate an SAH. The nylon thread was removed, the ECA was occluded at the carotid bifurcation, and the silk thread of the CCA occlusion was released and allowed to re-perfuse.

Intra-vital TPLSM

The two-photon microscope consisted of an upright microscope (BX61WI, Olympus, Tokyo, Japan) attached to a mode-locked titanium-sapphire laser system (Chameleon Vision II, Coherent, Tokyo, Japan) that could achieve a 140-fs pulse width and an 80-MHz repetition rate with 17-W pump power at 820 nm (rhodamine 6G) and 920 nm (Qdot 655) for capillary line scanning. Images were acquired with a scanning unit (FV1000, Olympus, Tokyo) using Fluoview™ software (FV10-ASW, version 2.0, Olympus, Tokyo, Japan) and a water immersion 25× objective (XLPLN25 × WMP, NA 1.05). Fluorescent emission was detected by an external photomultiplier tube (R3896, Hamamatsu Photonics,

Hamamatsu, Japan) after passing through an infrared blocking filter (685-nm cutoff) and an emission filter (570–625 nm for rhodamine 6G; 641–675 nm for Qdot 655).

Superimposed TPLSM images reveal the cortical microvasculature consisting of arterioles, capillaries, and venules. Each image is the sum of 13 slices at depths of 0–120 μm from the cerebral surface (slice interval, 10 μm) before SAH and at 60 min after SAH, and images at 100 μm depth are also shown (Fig. 1a, b).

Line-scan method

Blood cell velocities in capillaries were measured with a line-scan method, using Fluoview software. A line-scan image was assembled sequentially line by line with a speed of 2–3 ms per line (depending on the length of a scan line), 1 line per pixel. Pixel sizes were 0.331 μm (spatial distance) and 2–3 ms (temporal distance). In one line-scan analysis, an image was scanned with lines from top to bottom, and its image size was 100–200 pixels (spatial distance) × 1000 pixels (temporal size). Thus, 1000 lines represented 1000 pixels. The width of a blood cell spans several scanned lines. The fluorescence of a leukocyte is wider than that of a platelet in a scanned line. Thus, the line of a leukocyte is bolder than that of a platelet. The velocity of a blood cell can be calculated from a line-scan image (Fig. 1c, d).

Experimental protocols

A small bolus of 15 μl of Qdot 655 nanocrystals (Q21021MP, Invitrogen, Co., Carlsbad, CA) with 85 μl of saline was injected slowly in order to visualize the cerebral microvasculature. We found penetrating arterioles from the pial arteries on the cerebral surface and traced along a penetrating arteriole to find a branched precapillary arteriole at about 100 μm deep. We recognized and recorded capillaries, venules, and penetrating and precapillary arterioles surrounded by astrocyte end feet in the GFAP-GFP transgenic mice.

First, following Qdot administration, capillary networks were recorded before SAH and 60 min after SAH and also recorded at 0 min and 60 min after a sham operation. Next, an experiment was performed to measure blood cell velocities in the randomly selected capillary 60 min after SAH. Then, 50 μl of 0.02 % rhodamine 6G (Sigma-Aldrich Chemicals, St. Louis, MO) was administered intravenously, followed by a continuous infusion (1 ml/h) of 0.02 % rhodamine 6G at the same concentration for 10 min. The rhodamine 6G-labeled leukocytes and platelets and unlabeled red blood cells (RBCs) were analyzed with a line-scan method and recorded in eight randomly selected capillary segments.

Seventeen mice were assigned to one of three experimental groups: (1) sham surgery normal group ($n = 6$), (2) SAH group ($n = 7$), or (3) P-selectin treated SAH (SAH/Psel) group ($n = 4$). In the SAH/Psel group, a monoclonal antibody (mAb) directed against P-selectin (RB 40.34, 2 mg/kg) was administered intravenously 5 min after SAH to inhibit leukocyte rolling and platelet-leukocyte interactions. In all groups, velocities of leukocytes, RBCs, and platelets were quantified in capillaries at the precapillary arteriole branching level, about 100 μm from the brain surface, using the line-scan method, 60 min after SAH. In eight capillaries of each mouse, images with the line-scan method were recorded. At the end of the experiments, the skull base was opened, and the SAH spread was observed.

Video analysis

After the experiments, we analyzed the data and measured velocities with recorded images. The randomly selected eight capillary segments were also evaluated for leukocyte, RBC, and platelet flow velocities 60 min after SAH with the line-scan method, using Fluoview software (version FV10-ASW, Olympus, Tokyo). In one line scan, velocities of five cells were averaged. If there were only two or three cells in a line scan, then two or three velocities were averaged. In some capillaries, the line scans were repeated ten times to observe further changes in capillary flow after SAH. Fluorescent lines were counted in each line-scan analysis, and the capillary flow was estimated. Unlabeled RBC lines could not be counted because they were often not clear lines.

Statistics

Data were analyzed using the analysis of variance and Fisher's post hoc test or paired t-test as appropriate. The data are reported as mean ± SD. Statistical significance was set at a P value < 0.05.

Results

In vivo images using TPLSM

Capillaries were well recognized before SAH, but few and narrower capillaries were recognized 60 min after SAH (Fig. 1a, b). Thicker arteries and veins were recognized 60 min after SAH. The superimposed images show the capillary networks, and the cross sections represent either a penetrating arteriole or venule. Sixty minutes after SAH, the cortical capillary networks were broken, and examination of discontinuous capillaries revealed the disappearance of flow (most longitudinal sections). Recognized capillaries were narrower than before SAH. A penetrating arteriole branched into a precapillary arteriole first from the cerebral surface at a depth of about 100 μm.
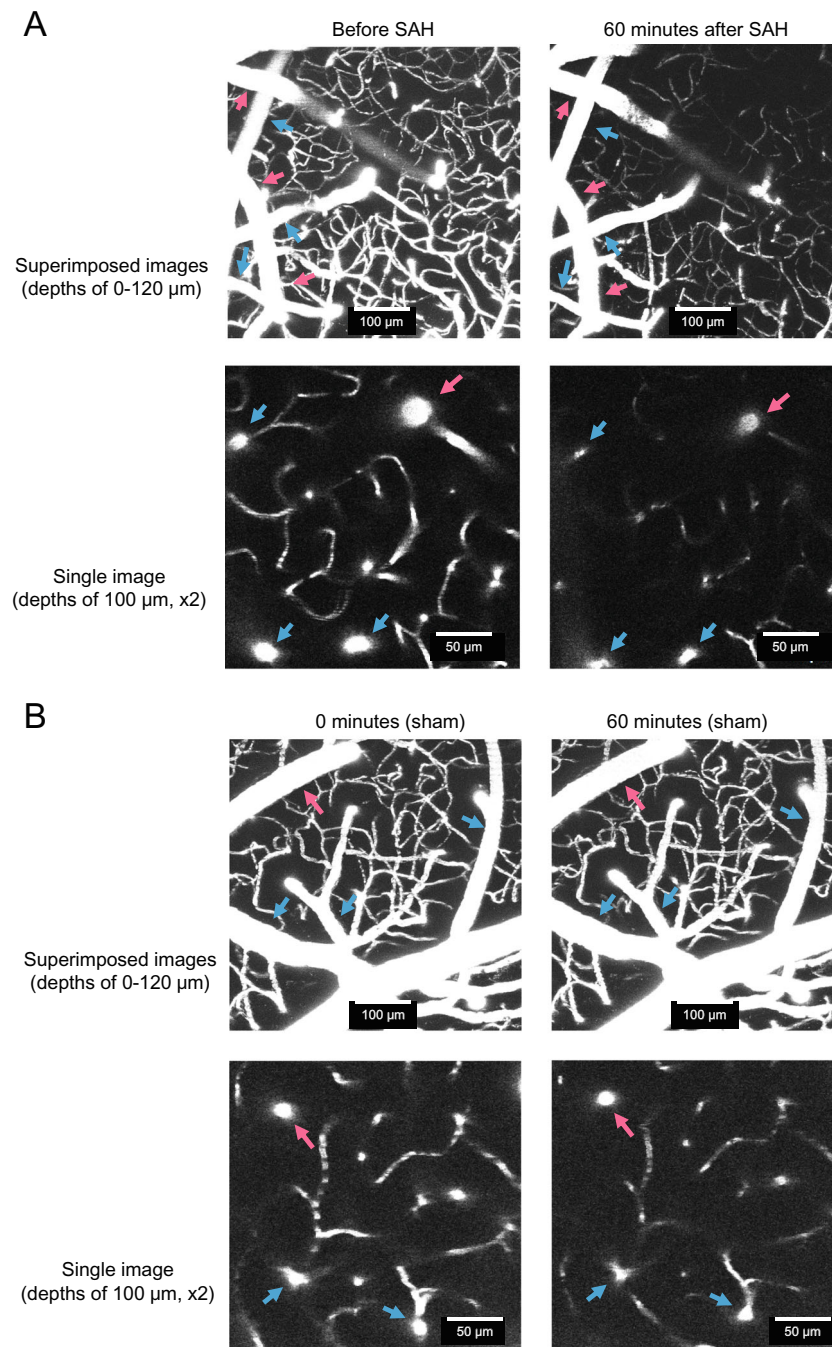
Fig. 1 Cortical microvasculature consisting of arterioles, capillaries, and venules. **a** The upper picture is the sum of 13 slices at depths of 0–120 μm from the cerebral surface (slice interval, 10 μm) before subarachnoid hemorrhage (SAH) and 60 min after SAH in the SAH group. The lower picture is one slice at a depth of 100 μm before SAH and 60 min after SAH. Sixty minutes after SAH, the cortical capillary networks are broken and discontinuous compared to a sham group (B). Red arrow: penetrating arteriole; blue arrow: venule. **b** The upper picture is the sum of 13 slices at depths of 0–120 μm from the cerebral surface (slice interval, 10 μm) after sham operation and 60 min later in the sham group. The lower picture is one slice at a depth of 100 μm after sham operation and 60 min later. **c** Representative image of a line-scan analysis (right) and its capillary in the microscopic image at a depth of 100 μm (left). **d** Scheme of a line-scan method; upper images show a flowing cell and middle images show an adherent cell. A blood cell is shown at six time points in each of the six sequentially scanned lines. The six lines are laid out to make a slope line of fluorescent cells (lower left: flowing; lower right: flowing to adhesion). Using the slope line, the velocities can be calculated

Flow velocity of blood cells in capillaries

Line-scan images were recorded following continuous in-fusion of rhodamine 6G for measurement of velocities of blood cells using Fluoview software (Fig. 1c). Leukocytes and platelets are visualized by fluorescently labeling these with rhodamine 6G. Large fluorescent leukocytes, small fluorescent platelets, and unlabeled (black) RBCs were
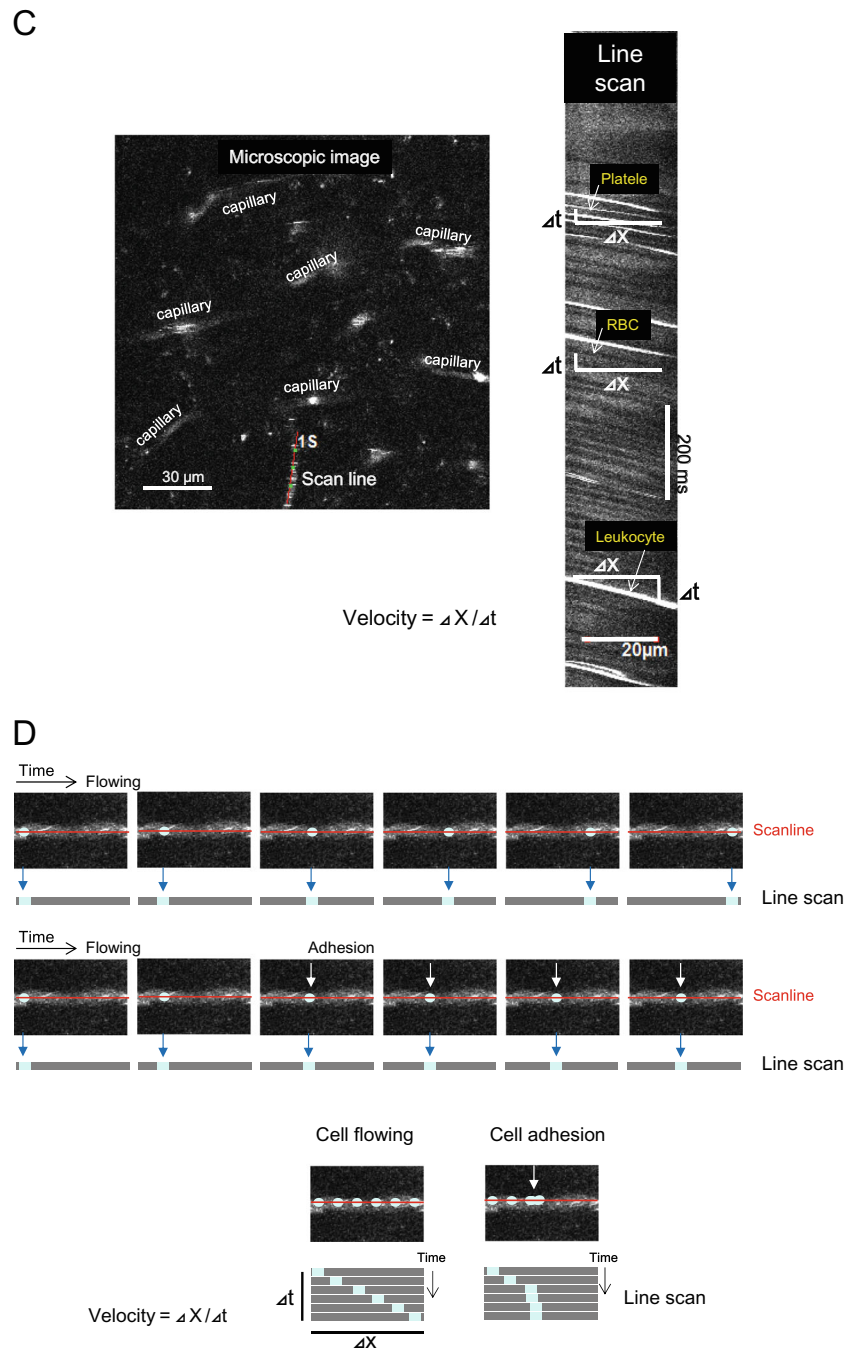
C

Velocity = ⊿X / ⊿t

D

Velocity = ⊿X / ⊿t

Fig. 1 (continued)

observed (Figs. 1c and 2). However, these flows were disturbed after SAH. The sharp slope of the line scan indicated low velocity. When the leukocytes rolled and adhered to the capillary endothelial cells, other blood cell flow also decreased and eventually disappeared. In one area observed with TPLSM, flow decreased or stopped in many capillaries (Fig. 2b). In a representative section of these capillaries, capillary flow was demonstrated for a while. Velocity of cell flow (slope of the line scan) changed

depending on each line scan. It appeared that the larger the slope was, the slower the velocity. It appeared also that the larger the slope was, the lower the cell number if the cell density was the same between the line scans (Fig. 2c). Then, rolling or adherent leukocytes prevented the cell flow, and cell flow changed and stopped (Fig. 2c). We hypothesized that fluorescent points (Fig. 2b, small arrows) represented adherent leukocytes preventing capillary flow. One of the reasons why the capillary flow
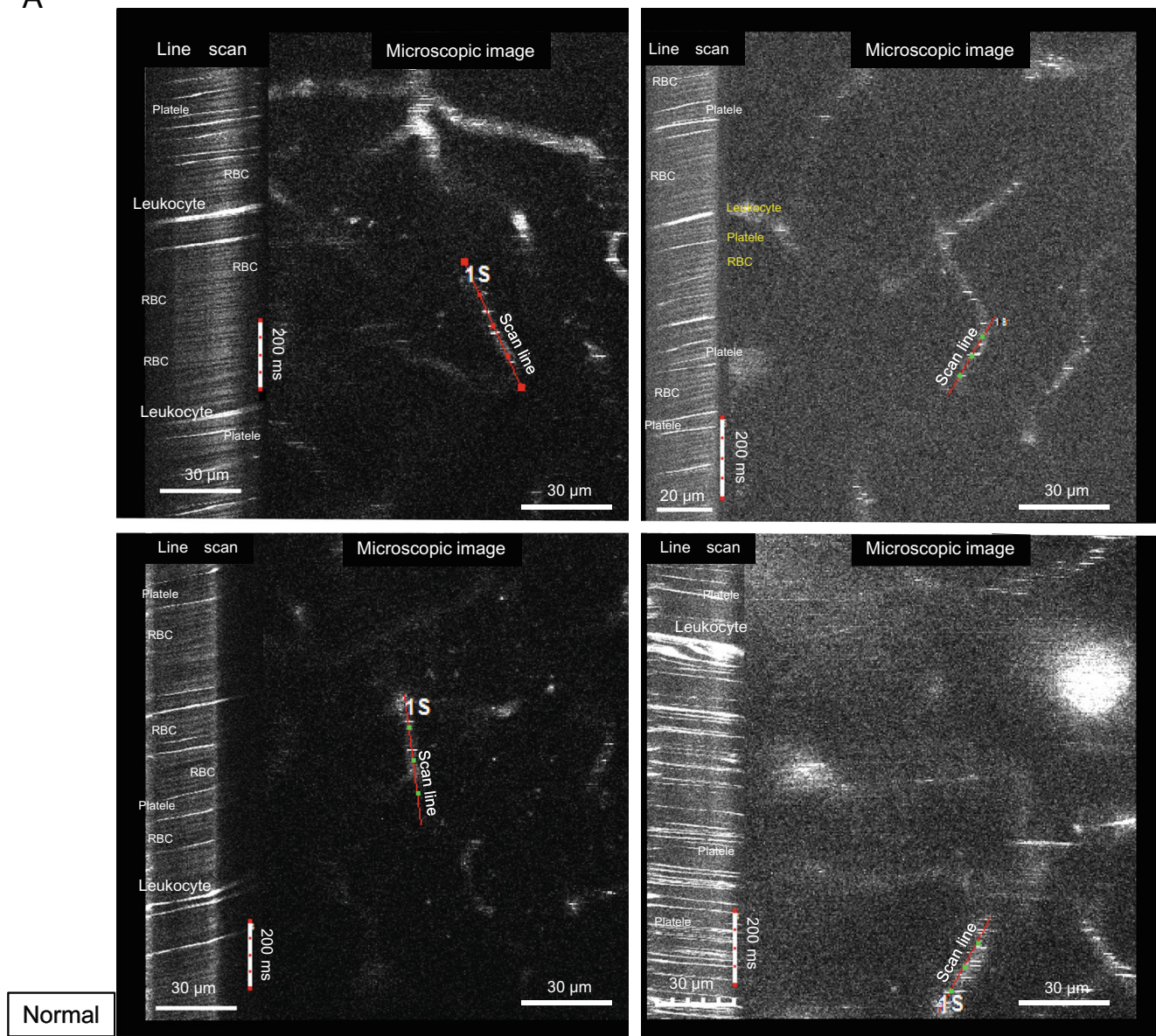
Fig. 2 Line-scan analyses of capillaries at a depth of about 100 μm. **a** Four line scans in the sham group; bold white lines are leukocytes. Fine white lines are platelets. Non-fluorescent black lines are red blood cells (RBCs). Scan line (red line) in the right microscopic image: position of line-scan analysis in a capillary. Leukocytes flow more slowly and platelets flow faster than the other cells. Leukocytes hardly pass other cells in line scans (**A**, **B**, yellow letters). **b** Line scans in a mouse 60 min after SAH. In a representative microscopic field (white square), every slope of each line scan is larger compared to a sham group (**A**). An adherent leukocyte prevents other blood cells from flowing. In the observed microscopic image (white square), other white spot areas may show the flow-preventing adherent leukocytes (small white arrows). **c** In a capillary (one of the capillaries in **B**), a time course of line scans for 10 min (1–7); slope of each line-scan changes from scan to scan (1–4). Some flowing leukocytes roll and adhere. The rolling and adherent leukocytes prevent cells from flowing (5). After a leukocyte adheres, flowing cells are not observed (5, 6). A few minutes later, more leukocytes adhere (7)

disappeared after SAH (Fig. 1a) was the adhesion of leukocytes. Excluding capillaries with no reflow after SAH, flow velocities of leukocytes, RBCs, and platelets decreased significantly compared to those in the sham group, and the cell count also decreased significantly (Fig. 3).

The velocities of leukocytes were slower than those of RBCs and platelets in the sham, SAH, and SAH/Psel groups, and the velocities of platelets were faster than those of RBCs and leukocytes in each group as analyzed by the paired *t*-test. In each line scan, a leukocyte seemed to flow more slowly and a platelet seemed to flow more quickly than the other cells (Figs. 1c and 2a, B, yellow letters). Individual cells did not pass other cells in line scans. The cell count of capillaries showed a similar
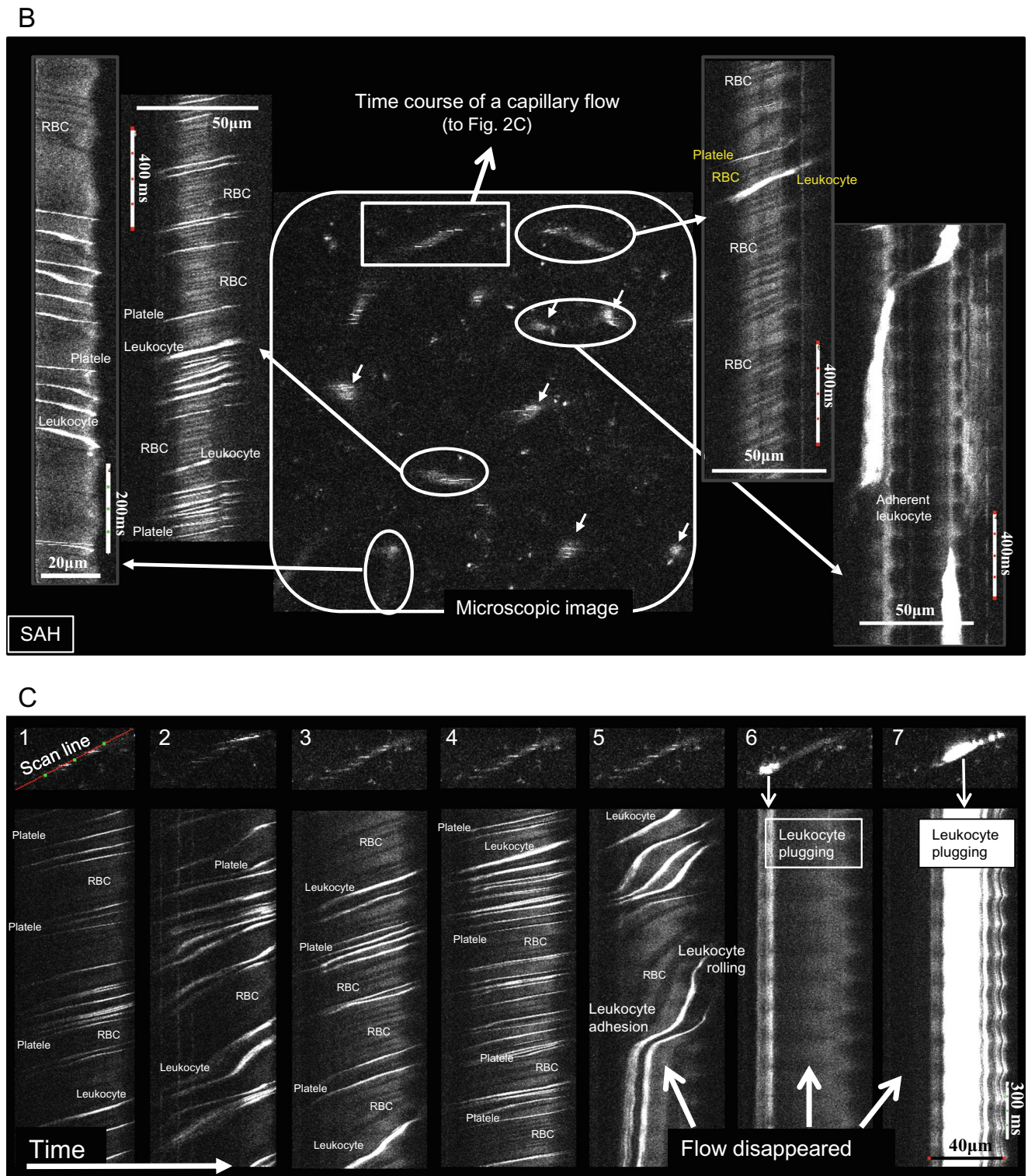
Fig. 2 (continued)

distribution to the velocity (Fig. 3b). In a line scan, the faster the cell velocity was, the lower the cell number (Fig. 2c). This cell count reflects the fluorescent cells (platelets and leukocytes), but may represent overall cerebral blood flow.

Effects of treatment with mAb against P-selectin on SAH-induced microcirculatory impairment

To examine the molecular mechanism of the no-reflow phenomenon in capillaries and whether adherent

Fig. 3 Velocities (**A**) of leukocytes, RBCs, and platelets in capillaries and cell count of leukocytes and platelets (**B**). In the SAH group, the velocities and cell counts are lower compared to the sham group. In P-selectin-treated mice with SAH, the velocities tend to recover. Sham: sham operation group; SAH: SAH group; SAH/Psel: SAH and P-selectin antibody administration group; *, < 0.05 vs. sham group; #, < 0.05 vs. SAH group; ¶, < 0.05 vs. RBC or platelet in each group; §, < 0.05 vs. RBC or leukocyte in each group
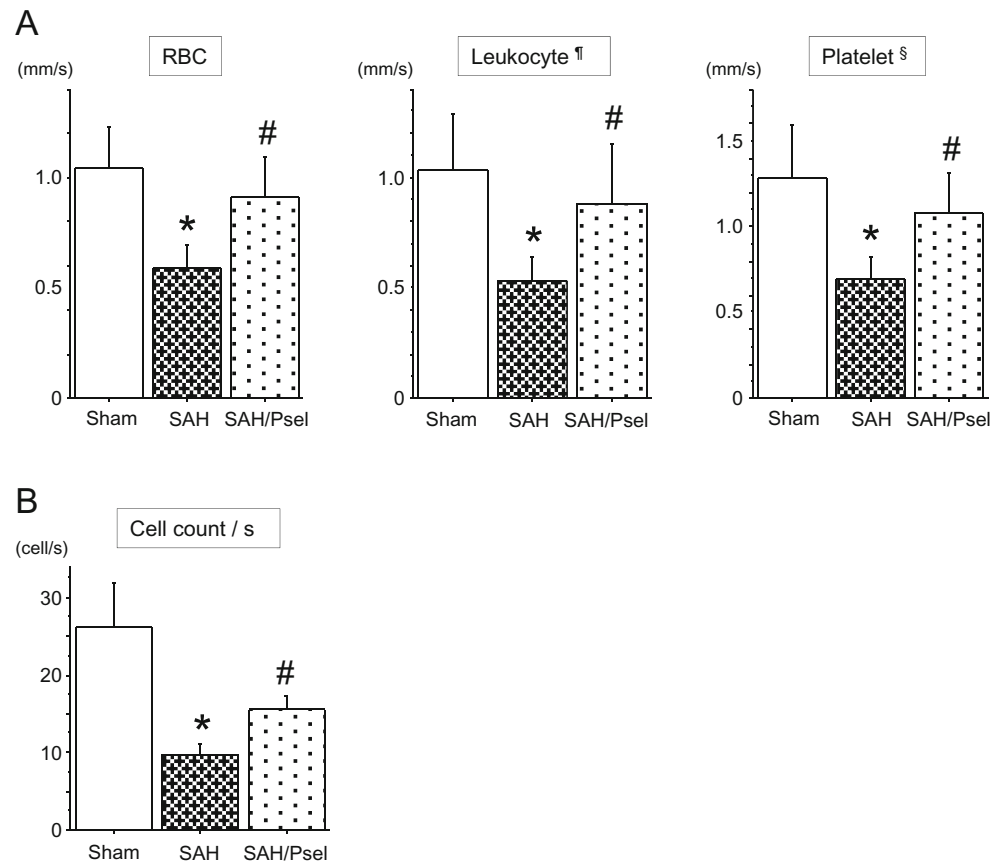
leukocytes were the cause, we used P-selectin mAb. In mice treated with a P-selectin mAb after SAH, flow velocities of leukocytes, RBCs, and platelets increased significantly compared to the velocities of the non-P-selectin mAb-treated SAH group. The fluorescent cell count also increased compared to the SAH group (Fig. 3).

Physiological parameters

Blood pressure (BP) at each time point and blood gas analysis data after experimental measurements are shown in Table 1. The BP and blood gas analysis data did not differ significantly between the two groups.

Discussion

ICP increases after SAH, and extensive brain ischemia is induced, leading to acute brain injury. This acute brain injury worsens the patient's clinical status at the onset and induces inflammatory responses, which have also been induced by puncture or injury of a cerebral artery in animal SAH models [2, 3, 8, 9, 12, 20, 22, 24, 25, 30, 31, 36, 37]. Recently, an endovascular perforation model of rats or mice with a nylon thread has often been used and has been shown to represent the actual change in flow dynamics after clinical SAH [3, 8, 9, 20, 24, 25, 30, 31], and with this model, the cerebral microcirculation and the pathophysiology of SAH has been investigated [8, 20]. In this report, we first observed the cortical

Table 1 Blood pressure and blood gas analysis

	Blood pressure (mmHg)	Blood gas analysis		
		pH	pO2 (mmHg)	pCO2 (mmHg)
Sham	92.4 ± 10.1	7.268 ± 0.071	85.6 ± 16.3	41.7 ± 5.2
SAH	99.7 ± 9.5	7.228 ± 0.049	87.8 ± 10.2	42.3 ± 7.6
SAH/Psel	96.8 ± 11.6	7.283 ± 0.092	92.8 ± 11.5	44.1 ± 5.2

microcirculation after SAH with TPLSM following Qdot administration and next focused on capillary flow 60 min after SAH with a line-scan method using TPLSM following rhodamine 6G administration.

When a sudden increase in ICP begins after SAH at the skull base, all venules and capillaries are compressed, their flow decreases, and cerebral ischemic damage is induced, which affects the whole brain, and is followed by inflammatory responses [10, 20, 24, 25, 30, 34, 35]. We have already reported platelet-leukocyte-endothelial cell interactions at the cerebral surface 120 min after SAH. These observations from the cerebral surface after SAH at the skull base are representative of whole-brain investigation because microcirculatory disturbances at the cerebral surface might not be severe compared to that at the skull base or the within the brain between the skull base and cerebral surface, and it is also difficult to observe skull base microcirculation. In this study, to better understand the pathophysiologic mechanisms after SAH, we used TPLSM to directly observe the microcirculatory phenomena in the cortex of mice after SAH (at about a 100-μm depth). The blood cell velocities in the capillaries decreased significantly compared to those of a sham group, and rolling and adherent leukocytes were frequently detected in cortical capillaries, as one of the inflammatory responses following SAH. The rolling and adherent leukocytes plugged capillaries, and the plugging leukocytes prevented flow of other blood cells. With a line-scan method using TPLSM, these phenomena were first clearly observed after SAH.

This no-reflow phenomenon had already been proposed as an important pathophysiologic mechanism of postischemic injury [1, 5, 39, 40], and it is believed that the causes of the no-reflow phenomenon are platelet activation, fibrin formation, and leukocyte adhesion [6, 14, 26]. However, it is not clear whether an individual leukocyte actually obstructs a capillary [7], although leukocyte rolling and adhesion can be easily observed in the microvasculature of the cerebral surface with an intra-vital fluorescence microscope [7, 17–20, 39]. Recently, using TPLSM, it was reported that flow stagnation because of leukocyte plugging was frequently observed in the deep cortical capillaries in a state of chronic cerebral hypoperfusion [40]. To specifically observe the cortical microcirculation, not the cerebral surface, TPLSM is very useful compared to conventional fluorescence microscopy [11, 16, 27, 28, 32]. The cortical capillary flow can be easily calculated with the line-scan method using TPLSM [15, 23, 32]. Moreover, the no-reflow phenomenon after SAH has been discussed as a mechanism of acute brain injury [2, 37, 38], but it has never been demonstrated in SAH models in vivo, using a conventional in vivo fluorescein microscope. Even if a leukocyte plugs a capillary, the plasma flow may be maintained, and a capillary may be observed with a fluorescein microscope. In this study using the line-scan method of TPSLM, leukocyte plugging was frequently observed in the cortical capillaries after SAH, and other cell flow was not observed after leukocyte plugging, which supports the no-reflow phenomenon following cerebral ischemia.

This no-reflow phenomenon is one of the elements of cortical microcirculatory disturbance immediately after SAH. Moreover, the decrease of the blood cell velocities in capillaries recovered after administration of anti-P-selectin antibody. Similar recovery in capillaries has been reported in the skeletal muscle [21] and lung [33]. P-selectin/P-selectin glycoprotein ligand-1 (PSGL-1) interactions have been implicated as mediators of blood cell adhesion, and leukocyte PSGL-1 binds to endothelial P-selectin to mediate leukocyte rolling in veins. The use of a blocking antibody targeted against P-selectin attenuates this leukocyte rolling and subsequent adhesion. P-selectin may be induced on mouse brain capillary endothelial cells [4], and then P-selectin can directly mediate leukocyte rolling in capillaries. On the other hand, this P-selectin-mediated leukocyte-endothelial cell interaction may be a phenomenon induced by inflammatory responses in postcapillary venules, similar to ischemia/reperfusion injury, which we have observed and reported to occur 2 h after SAH [20]. In this case, capillary flow is recovered by improvement of venous flow following the washout of rolling and adherent leukocytes after administration of P-selectin antibody. Early P-selectin-mediated inflammatory responses after SAH can begin when SAH occurs, because P-selectin is stored in granules within the endothelial cells (Weibel-Palade bodies) and can be mobilized rapidly to the cell surface of endothelial cells [29] without upregulation of P-selectin on the endothelium. We have previously observed platelet-leukocyte-endothelial cell interactions in cerebral venules, which were inhibited by anti-P-selectin antibody, in several models of inflammation, ischemia/reperfusion [18, 19], hypercholesterolemia [17], and SAH [20]. The activated leukocyte may adhere and plug in the capillary after SAH.

We believe that one of the most important factors for the initiation of the inflammatory response following SAH might be the sudden increase in ICP and prolonged decrease in CBF because the slow injection of blood into the cisterna magna did not increase the ICP and did not induce platelet-leukocyte-endothelial cell interactions [20]. The disturbance of the cortical capillary flow may be induced by a sudden increase in ICP in patients with SAH of different grades and kept by a persistently elevated ICP in patients with poor SAH grades. In our study, observing the line-scan images, leukocytes flow more slowly than other cells, other cells hardly pass the leukocytes, and leukocytes plugged after SAH. Leukocyte flow may be the rate-limiting step for capillary flow. These inflammatory responses and leukocyte motility characteristics require further investigation with a focus on the development of clinical treatments during the acute phase of SAH in order to produce better clinical outcomes. During the acute phase after SAH, anti-

inflammatory therapy may be an important method for patients with a poor SAH grade to recover more fully.

In summary, we first observed the microcirculation in the cortex immediately after SAH with a line-scan method using TPLSM and reported the cortical microcirculatory disturbance induced by leukocyte plugging, i.e., the no-reflow phenomenon after SAH. We present novel data that support the hypothesis that P-selectin mediates microcirculatory disturbance in capillaries following SAH.

Compliance with ethical standards

Conflict of interest None.

Ethical approval All procedures performed in studies involving animals were in accordance with the ethical standards of the Keio University Animal Care and Use Committee (12070–2).

References

1. Ames A III, Wright RL, Kowada M, Thurston JM, Majno G (1968) Cerebral ischemia II. The no-reflow phenomenon. Am J Pathol 52(2):437–453

2. Asano T, Sano K (1977) Pathogenetic role of no-reflow phenomenon in experimental subarachnoid hemorrhage in dogs. J Neurosurg 46(4):454–466

3. Bederson JB, Germano IM, Guarino L (1995) Cortical blood flow and cerebral perfusion pressure in a new noncraniotomy model of subarachnoid hemorrhage in the rat. Stroke 26(6):1086–1092

4. Coisne C, Faveeuw C, Delplace Y, Dehoyck L, Miller F, Cecchelli R, Dehouck L (2006) Differential expression of selectins by mouse brain capillary endothelial cells in vitro in response to distinct inflammatory stimuli. Neurosci Lett 392(3):216–220

5. del Zoppo GJ, Schmid-schoenbein GW, Mori E, Copeland BR, Chang C-M (1991) Polymorphonuclear leukocytes occlude capillaries following middle cerebral artery occlusion and reperfusion in baboons. Stroke 22(10):1276–1283

6. del Zoppo GJ, Hallenbeck JM (2000) Advances in the vascular pathophysiology of ischemic stroke. Thromb Res 98(3):V73–V81

7. Dirnagl U, Niwa K, Sixt G, Villringer A (1994) Cortical hypoperfusion after global forebrain ischemia in rats is not caused by microvascular leukocyte plugging. Stroke 25(5):1028–1038

8. Friedrich B, Mueller F, Feiler S, Schoeller K, Plesnila N (2012) Experimental subarachnoid hemorrhage causes early and long-lasting microarterial constriction and microthrombosis: an in-vivo microscopy study. J Cereb Blood Flow Metab 32(3):447–455

9. Friedrich V, Flores R, Muller A, Sehba FA (2010) Escape of intraluminal platelets into brain parenchyma after subarachnoid hemorrhage. Neuroscience 165(3):968–975

10. Germano A, d'Avella D, Cicciarello R, Hayes RL, Tomasello F (1992) Blood–brain barrier permeability changes after experimental subarachnoid hemorrhage. Neurosurgery 30(6):882–886

11. Girouard H, Iadecola C (2006) Neurovascular coupling in the normal brain and in hypertension, stroke, and Alzheimer disease. J Appl Physiol 100(1):328–335

12. Hayakawa T, Waltz AG (1977) Experimental subarachnoid hemorrhage from a middle cerebral artery. Neurologic deficits, intracranial pressures, blood pressures, and pulse rates. Stroke 8(4):421–426

13. Herz DA, Baez S, Shulman K (1975) Pial microcirculation in subarachnoid hemorrhage. Stroke 6(4):417–424

14. Huang J, Upadhyay UM, Tamargo RJ (2006) Inflammation in stroke and focal cerebral ischemia. Surg Neurol 66(3):232–245

15. Huang JY, Li LT, Wang H, Liu SS, Lu YM, Liao MH, Tao RR, Hong LJ, Fukunaga K, Chen Z, Wilcon CS, Lai EY, Han F (2014) In vivo two-photon fluorescence microscopy reveals disturbed cerebral capillary blood flow and increased susceptibility to ischemic insults in diabetic mice. CNS Neurosci Ther 20(9):816–822

16. Iadecola C, Nedergaard M (2007) Glial regulation of the cerebral microvasculature. Nat Neurosci 10(11):1369–1376

17. Ishikawa M, Stokes KY, Zhang JH, Nanda A, Granger DN (2004) Cerebral microvascular responses to hypercholesterolemia Role of NADPH oxidase and P-selectin. Circ Res 94(2):239–244

18. Ishikawa M, Vowinkel T, Stokes KY, Arumugan TV, Yilmaz G, Nanda A, Zhang JH, Granger DN (2005) CD40/CD40L signaling in mouse cerebral microvasculature after focal ischemia/.reperfusion. Circulation 111(13):1690–1696

19. Ishikawa M, Sekizuka E, Yamagchi N, Nakadate H, Terao S, Granger DN, Minamitani H (2007) Angiotensin II type 1 receptor signaling contributes to platelet-leukocyte-endothelial cell interactions in the cerebral microvasculature. Am J Physiol Heart Circ Physiol 292(5):H2306–H2315

20. Ishikawa M, Kusaka G, Yamaguchi N, Sekizuka E, Nakadate H, Minamitani H, Watanabe E (2009) Platelet and leukocyte adhesion in the microvasculature at the cerebral surface immediately after subarachnoid hemorrhage. Neurosurgery 64(3):546–554

21. Jerome SN, Dore M, Paulson JC, Smithi CW, Korthuis RJ (1994) P-selectin and ICAM-1-dependent adherence reactions: role in the genesis of postischemic no-reflow. Am J Physiol 266(4):H1316–H1321

22. Kamiya K, Kuyama H, Symon L (1983) An experimental study of the acute stage of subarachnoid hemorrhage. J Neurosurg 59(6): 917–924

23. Kleinfeld D, Mitra PP, Helmchen F, Denk W (1998) Fluctuations and stimulus-induced changes in blood flow observed in individual capillaries in layers 2 through 4 of rat neocortex. Proc Natl Acad Sci U S A 95(26):15741–15746

24. Kusaka G, Ishikawa M, Nanda A, Neil Granger D, Zhang JH (2004) Signaling pathways for early brain injury after subarachnoid hemorrhage. J Cereb Brain Flow Metab 24(8):916–925

25. Li Z, Liang G, Ma T, Li J, Wang P, Liu L, Xue Y (2015) Blood-brain barrier permeability change and regulation mechanism after subarachnoid hemorrhage. Metab Brain Dis 30(2):597–603

26. Mori E, del Zoppo GJ, Chambers JD, Copeland BR, Arfors KE (1992) Inhibition of polymorphonuclear leukocyte adherence suppresses no-reflow after focal cerebral ischemia in baboons. Stroke 23(5):712–718

27. Morikawa T, Kajimura M, Nakamura T, Hishiki T, Nakanishi T, Yukutake Y, Nagahata Y, Ishikawa M, Hattori K, Takenouchi T, Takahashi T, Ishii I, Matsubara K, Kabe Y, Uchiyama S, Nagata E, Gadalla MM, Snyder SH, Suematsu M (2012) Hypoxic regulation of the cerebral microcirculation is mediated by a carbon monoxide-sensitive hydrogen sulfide pathway. PNAS 109(4): 1293–1298

28. Nakamura T, Kajimura M, Morikawa T, Hattori K, Ishikawa M, Yukutake Y, Uchiyama S-I, Suematsu M (2011) Acute CO2-independent vasodilatation of penetrating and pre-capillary arterioles in mouse cerebral parenchyma upon hypoxia revealed by a thinned-skull window method. Acta Physiol 203(1):187–196

29. Pinsky DJ, Naka Y, Liao H, Oz MC, Wagner DD, Mayadas TN, Johnson RC, Hynes RO, Heath M, Lawson CA, Stem DM (1996) Hypoxia-induced exocytosis of endothelial cell Weibel-Palade bodies. A mechanism for rapid neutrophil recruitment after cardiac preservation. J Clin Invest 97(2):493–500

30. Schoeller K, Trinke A, Klopotowski M, Thal SC, Plesnila N, Trabold R, HamannGF S-ER, Zausinger S (2007) Characterization of microvascular basal lamina damage and blood–brain barrier dysfunction following subarachnoid hemorrhage in rats. Brain Res 1142:237–246

31. Sehba FA, Friedrich V, Makonnen G, Bederson JB (2007) Acute cerebral vascular injury after subarachnoid hemorrhage and its prevention by administration of a nitric oxide donor. J Neurosurg 106(2):321–329

32. Shih AY, Driscoll JD, Drew PJ, Nishimura N, Schaffer CB, Kleinfeld D (2012) Two-photon microscopy as a tool to study blood flow and neurovascular coupling in the rodent brain. J Cereb Blood Flow Metab 32(7):1277–1309

33. Sikora L, Johansson ACM, Rao SP, Hughes GK, Broide DH, Sriramarao P (2003) A murine model to study leukocyte rolling and intravascular trafficking in lung microvessels. Am J Pathol 162(6):2019–2028

34. Trojanowski T (1982) Blood–brain barrier changes after experimental subarachnoid haemorrhage. Acta Neurochir (Wien) 60(1–2):45–54

35. Trojanowski T (1982) Experimental subarachnoid haemorrhage. Part II: extravasation volume and dynamics of subarachnoid arterial bleeding in cats. Acta Neurochir 64(1–2):103–108

36. Trojanowski T (1984) Early effects of experimental arterial subarachnoid haemorrhage on the cerebral circulation. Part I: experimental subarachnoid haemorrhage in cat and its pathophysiological effects methods of regional cerebral blood flow measurement and evaluation of microcirculation. Acta Neurochir (Wien) 72(1–2):79–94

37. Trojanowski T (1984) Early effects of experimental arterial subarachnoid haemorrhage on the cerebral circulation. Part II: regional cerebral blood flow and cerebral microcirculation after experimental subarachnoid haemorrhage. Acta Neurochir (Wien) 72(3–4): 241–259

38. Trojanowski T (2008) How intracranial aneurysm rupture damages the brain. Interv Neuroradiol 14(1):9–12

39. Villringer A, Dirnagl U, Them A, Schuerer L, Krombach F, Einhaeupl KM (1991) Imaging of leukocytes within the rat brain cortex in vivo. Microvasc Res 42(3):305–315

40. Yata K, Nishimura Y, Unekawa M, Tomita Y, Suzuki N, Tanaka T, Mizoguchi A, Tomimoto H (2014) In vivo imaging of the mouse neurovascular unit under chronic cerebral hypoperfusion. Stroke 45(12):3698–3703

Comments

The authors provided a very elegant study on the pathophysiology of the cortical microcirculation after subarachnoid hemorrhage (SAH) in a rodent model. They very clearly demonstrated that when a sudden increase of intracranial pressure (ICP) begins after SAH, blood cell velocities in the capillaries decrease significantly and "rolling" and adherent leukocytes plug capillaries, preventing other blood cells from flowing. According to the results here provided, this is the consequence of an ICP rise that determine the compression of capillaries and decrease of blood flow. This in turn causes cerebral ischemic damage and an inflammatory response. This study provides robust evidence about the subsistence of this pathophysiological event and interesting illustrations. Further studies to demonstrate the translational potential of these findings are warranted. In particular, it is true that an abrupt ICP rise is present after SAH. Nevertheless, this cortical dysfunction might be present only in severe SAH cases. I wonder whether it is the persistently elevated ICP, present in severe SAH grades, instead of an abrupt rise with a quick fall that plays a major role. An indication of the intensity and the duration of the ICP rise able to induce such microvessel paralysis would be desirable. Thus, the authors are invited to continue their studies and provide further data on this interesting issue.

Alfredo Conti
Messina, Italy